SUPPLEMENTAL METHODS

Microarray construction and validation. The microarray experiments in this study were performed using glass slides spotted with unique 70-mer oligonucleotides corresponding to all 835 annotated ORFs from the *R. prowazekii* genome sequence. 70-mer oligonucleotides were designed from these sequences by using ArrayOligoSelector (3). All 70-mer oligonucleotides were verified as specific for *R. prowazekii* and not *Mus musculus* (the host cell used for rickettsial infections) under the conditions of hybridization used in this study using the BLAST algorithm (1, 2). The arrays consisted of two unique 70-mer oligonucleotides for 666 *R. prowazekii* ORFs and, by necessity, a single unique oligonucleotide for the remaining 169 ORFs. The oligos were synthesized by using standard methods by Illumina (San Diego). The oligonucleotides were dissolved at a concentration of 50 mM in 3 × SSC with 0.75 M betaine and were printed in duplicate on MWG Epoxy slides (MWG Biotech, Ebersburg, Germany) by a locally constructed linear servo arrayer (after the DeRisi model) (4). The oligonucleotides were spotted in triplicate. In addition, oligonucleotide probes corresponding to 32 mouse genes were included as negative controls and oligonucleotide probes corresponding to 10 *Arabidopsis thaliana* genes (SpotReport® Oligo Array Validation System, Stratagene) were included as reaction controls. *A. thaliana* mRNA spikes (Stratagene) were mixed with RNA samples to assess cDNA synthesis and labeling efficiencies in each reaction.

As an initial array validation experiment, samples containing 1 and 4 μg of rickettsial total RNA taking from a single isolation were converted cDNA using random hexamers and labeled using the 3DNA Array 900MPX Detection system from Genisphere. The Genisphere detection system employs indirect labeling using fluorescent dendrimers subsequent to cDNA synthesis. In an independent experiment, the dyes were reversed to control for any labeling differences (technical replicates). The cDNA was hybridized to the microarray (in duplicate with a dye swap), labeled,

and analyzed without any normalization of the data other than background subtraction. Under these conditions, all rickettsial oligonucleotide probes were expected to show a four-fold difference in intensity between two samples. This analysis demonstrated that the rickettsial oligonucleotide probes on the microarray performed as expected giving an overall ratio of 4:1 (**Fig. S2**). In addition, the validation experiment showed that all probes demonstrated a significant hybridization signal (either a signal intensity > 200 or signal/local background ratio > 2) in the 1 μg RNA sample indicating that all 835 putative *R. prowazekii* mRNAs could be detected in our analyses. We also verified that there was minimal background hybridization from mouse RNA by labeling and hybridization mouse total RNA from a mock infection (pre-treated with MICROB*Enrich*) to the rickettsial microarray (data not shown). For all other microarray experiments, control and heat shock samples were hybridized to a glass slide microarray overnight (42 ^{o}C), labeled, and scanned at both high and low photomultiplier tube settings. The resulting values were corrected for background, normalized using a Lowess algorithm, and analyzed using Genespring 7.1 and Microsoft Excel.

Table S1. Quantitative RT-PCR Primer Sequences. [a]

RP042	
RT primer	5'-TTA GCA AAA ATG GGT AAA ACG AGA TAC-3'
Q-PCR forward primer	5'-AAT ATC GGC AAT AGC TGA AG-3'
Q-PCR reverse primer	5'-CGT GCT GAT CTA GAT TGT CC-3'
RP044	
RT primer	5'-TTA TAC TCC ATG GCG TTC TGC-3'
Q-PCR forward primer	5'-ATA CGA CCC TGA TCT TGA TG-3'
Q-PCR reverse primer	5'-TAT TCA TTG CAC AAC TAC CG-3'
RP626	
RT primer	5'-TTA GAA GTC CAT ACC ACC CAT G-3'
Q-PCR forward primer	5'-CCG AAA ATT ACA AAA GAT GG-3'
Q-PCR reverse primer	5'-GCT GCA ACC AAC TTA TTA CC-3'
RP629	
RT primer	5'-TTA AGG TTT TTT AAC TAC TTG TAC TGC AG-3'
Q-PCR forward primer	5'-AGC CTT AAA AGC CGA GAT TG-3'
Q-PCR reverse primer	5'-TCA TCT GCA CAC CGG AAA TA-3'

[a] All PCRs were run using the same conditions which included an initial denaturation step of 95 ^{o}C for 120 sec followed by cycling at 95 ^{o}C for 15 sec; 50 ^{o}C for 15 sec; 72 ^{o}C for 15 sec for a total of 40 cycles.

SUPPLEMENTAL FIGURE LEGENDS

FIG. S1. Purification and enrichment of total *R. prowazekii* RNA. (A) Total RNA from rickettsiae-infected L929 mouse fibroblast cells. (B) Rickettsiae-infected L929 cells were broken by ballistic shearing, rickettsiae purified by differential centrifugation and total RNA isolated. (C) Total RNA from panel (B) was further purified by Ambion's MICROB*Enrich*. (D) The rickettsial pellet isolated by differential centrifugation was further purified by centrifugation through 25% Renograffin and total RNA isolated. In all cases, RNA was extracted as described in Materials and Methods and total RNA (L-cell and rickettsial) quality and quantity was determined using an Agilent Bioanalyzer.

FIG. S2. Microarray validation. Total *R. prowazekii* RNA from a single extraction was used to prepare cDNA labeling reactions using 1 and 4 μg for microarray hybridization as described in Material and Methods. A background subtraction was performed and the data plotted with no other normalization. The data showed an expected four-fold difference between the two samples. The line of unity (ratio of 1) is shown in green flanked by two lines representing a two-fold change. All *R. prowazekii* mRNAs were tagged as present (either a signal intensity > 200 or signal/local background ratio >2) in both the 1 and 4 μg RNA samples.

FIG. S3. Verification of array results by quantitative RT-PCR. Panel (A) depicts a representative plot of qRT-PCR results for the heat shock gene RP044 under control (34 ^{o}C, closed squares) and heat shock (42 ^{o}C, open squares) conditions. Equal amounts of total rickettsial RNA from control and heat shock experiments (determined using the Agilent Bioanalyzer) were converted to cDNA using reverse primers specific to the genes of interest. The RT reactions were treated with RNaseH and serially diluted four-fold. qPCR was performed in duplicate on each dilution using a pair of

nested primers for each of the genes tested (both data points are shown on the representative plot). Cycle threshold (CT) was plotted against $\log_{10}$ template concentration. Linear regression analysis was used to determine reaction efficiency where $E = 10^{(-1/slope)}$ (5) and R^2 values are reported. Theoretical data are shown for a reaction working at optimal efficiency (closed diamonds); by definition, a PCR running at optimal efficiency will result in a doubling of product for every cycle run (E = 2) which is represented by a line with a slope of –3.3. Controls without the addition of RT were performed to confirm the absence of contaminating DNA. Panel (B) shows the qRT-PCR data from biological replicates 3 and 4 (additional RNA was available from these experiments). Using the protocol described above the average slope from multiple qPCR runs was used to determine a reaction efficiency (E) for each primer set (CV $\leq$ 0.1, standard deviations reported in the table). CT_i is the ordinate intercept of the linear regression for the control and heat shock samples. Fold induction was calculated as $E^{(CTi\ control - CTi\ heat\ shock)}$ (modified from (5)).

FIG. S1.

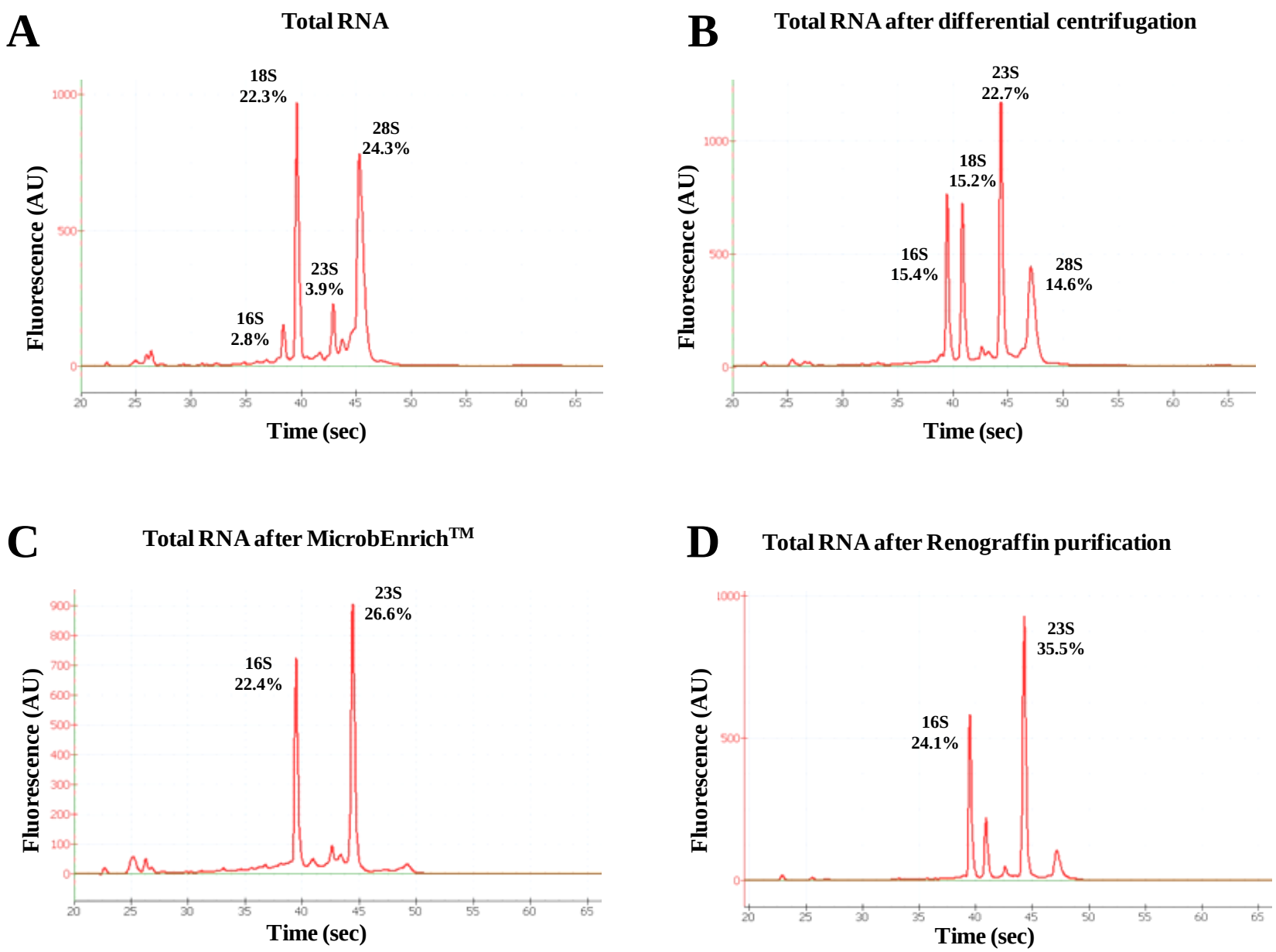
A
Total RNA
18S
22.3%
28S
24.3%
23S
3.9%
16S
2.8%
Fluorescence (AU)
Time (sec)
B
Total RNA after differential centrifugation
23S
22.7%
18S
15.2%
16S
15.4%
28S
14.6%
Fluorescence (AU)
Time (sec)
C
Total RNA after MicrobEnrich™
23S
26.6%
16S
22.4%
Fluorescence (AU)
Time (sec)
D
Total RNA after Renograffin purification
23S
35.5%
16S
24.1%
Fluorescence (AU)
Time (sec)

FIG. S2.

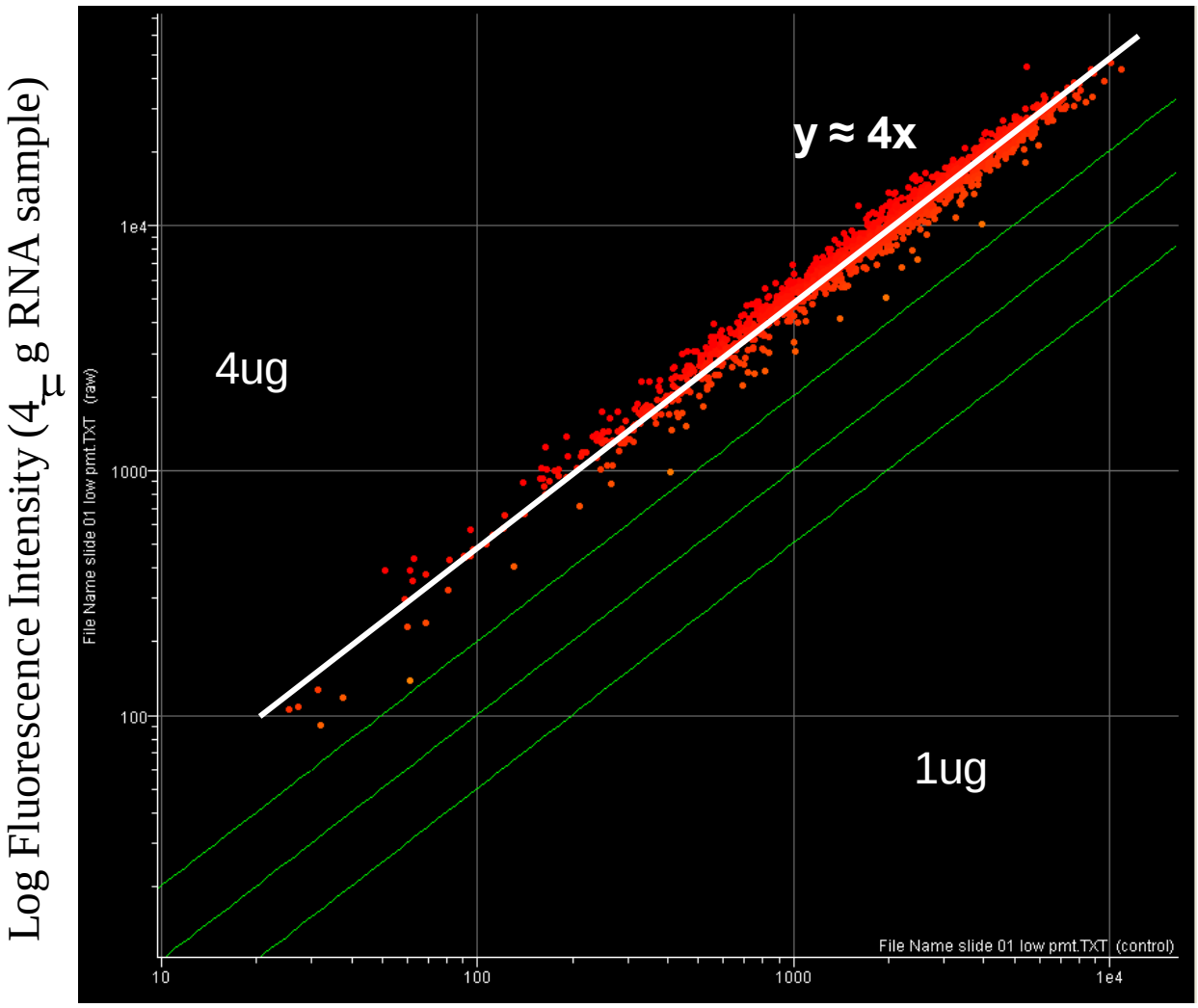
y ≈ 4x
4ug
1ug
1e4
1000
100
10
100
1000
1e4
File Name slide 01 low pmt.TXT (raw)
File Name slide 01 low pmt.TXT (control)
Log Fluorescence Intensity (4 μg RNA sample)
Log Fluorescence Intensity (1 μg RNA sample)

FIG. S3.

A

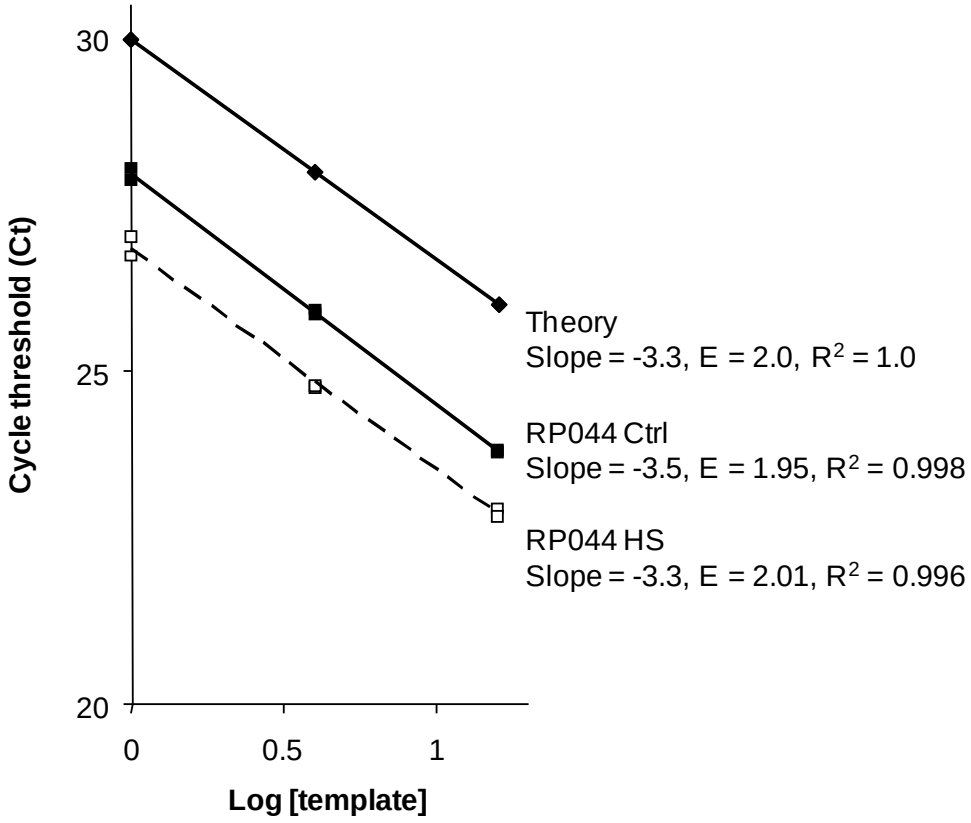

B

		Biological Replicate 3			Biological Replicate 4		
		CT_i			CT_i		
	Average Reaction Efficiency (E)	Control	Heat Shock	Fold Induction	Control	Heat Shock	Fold Induction
RP044	2.02 ± 0.08	24.19	22.32	3.7	23.80	22.84	2.0
RP626	2.21 ± 0.06	19.51	15.98	16.3	19.53	16.63	9.9
RP629	2.16 ± 0.15	20.74	20.17	1.6	22.40	20.93	3.1

SUPPLEMENTAL REFERENCES

1. **Altschul, S. F., W. Gish, W. Miller, E. W. Myers, and D. J. Lipman.** 1990. Basic local alignment search tool. J. Mol. Biol. **215:**403-10.

2. **Altschul, S. F., T. L. Madden, A. A. Schaffer, J. Zhang, Z. Zhang, W. Miller, and D. J. Lipman.** 1997. Gapped BLAST and PSI-BLAST: a new generation of protein database search programs. Nucleic Acids Res. **25:**3389-402.

3. **Bozdech, Z., J. Zhu, M. P. Joachimiak, F. E. Cohen, B. Pulliam, and J. L. DeRisi.** 2003. Expression profiling of the schizont and trophozoite stages of *Plasmodium falciparum* with a long-oligonucleotide microarray. Genome Biol. **4:**R9.

4. **Lashkari, D. A., J. L. DeRisi, J. H. McCusker, A. F. Namath, C. Gentile, S. Y. Hwang, P. O. Brown, and R. W. Davis.** 1997. Yeast microarrays for genome wide parallel genetic and gene expression analysis. Proc. Natl. Acad. Sci. U. S. A. **94:**13057-13062.

5. **Pfaffl, M. W.** 2001. A new mathematical model for relative quantification in real-time RT-PCR. Nucleic Acids Res. **29:**e45.